Eur. Phys. J. E (2012) **35**: 84
DOI 10.1140/epje/i2012-12084-y

THE EUROPEAN PHYSICAL JOURNAL E

Regular Article

Probability distributions for the run-and-tumble bacterial dynamics: An analogy to the Lorentz model

K. Martens[1], L. Angelani[2], R. Di Leonardo[2], and L. Bocquet[1,a]

[1] LPMCN, Université Lyon 1 and UMR CNRS 5586, 69622 Villeurbanne, France
[2] CNR-IPCF UOS Roma, Dipartimento di Fisica, Università Sapienza, I-00185 Roma, Italy

Received 1 May 2012 and Received in final form 22 June 2012
Published online: 14 September 2012 –

Abstract. In this paper, we exploit an analogy of the run-and-tumble process for bacterial motility with the Lorentz model of electron conduction in order to obtain analytical results for the intermediate scattering function. This allows to obtain an analytical result for the van Hove function in real space for two-dimensional systems. We furthermore consider the 2D circling motion of bacteria close to solid boundaries with tumbling, and show that the analogy to electron conduction in a magnetic field allows to predict the effective diffusion coefficient of the bacteria. The latter is shown to be reduced by the circling motion of the bacteria.

1 Introduction

The motility characteristics of *Escherichia coli* (*E. coli*) play a central role in the understanding of individual and collective behavior of self-propelling organisms. As highlighted in the seminal work of H. Berg [1], *E. coli* moves along straight trajectories, interrupted by quick reorientations, which at long times leads to a diffusive exploration of space. This swimming behavior was accounted for by H. Berg and co-workers by the so-called "run and tumble" model of bacterial motility, where a ballistic "run" phase at constant speed v_0 is followed by "tumble" periods, occurring with a fixed rate, say λ, and leading to a full randomization of the direction of motion [1–4]. In the long-time limit this leads to a Brownian-like behavior, with an effective diffusion coefficient of the organism, which scales as $D_{\rm eff} = v_0^2/d\lambda$ (d the dimension).

Although the idealized dynamics presented here does not account for interactions between bacteria, such as chemotactic, hydrodynamic and hard-core interaction, the "run and tumble" model acts as a paradigm for cell self-propulsion, and is at the root of numerous investigations of active microswimmers [5–10], and the consequences of which still continue to be explored.

Recently, it has been shown that a new imaging microscopy, namely differential dynamic microscopy (DDM), can provide a quantitative and robust characterization of some of the motility properties of a bacterial suspension. This method gives direct access to the intermediate scattering function (ISF) in Fourier space, $F(k,t) = \langle \exp[i\mathbf{k}\cdot\Delta\mathbf{R}_i(t)\rangle$ (with $\mathbf{R}_i(t)$ the trajectory of an individual swimmer), with unprecedented statistics and without the requirement of individual tracking of the swimming organisms [11,12]. However data analysis requires the *a priori* knowledge of the relevant $F(k,t)$ which is used for constructing the fitting function. According to the "run and tumble" model, a population of microswimmers behaves ballistically for short times, with a corresponding $F(k,t) = \sin(kv\,t)/kd\,t$ in 3D [11], while in the long time limit it approaches its diffusive counter-part $F(k,t) = \exp[-D_{\rm eff}k^2t]$. So far, experimental data have been interpreted using the ballistic approximation and observing that, in the accessed k-range, the isotropic distribution of bacterial swimming directions decorrelates the ISF on a time scale that is shorter than the average tumbling period. Moreover no general solution for $F(k,t)$ is known which takes into account the tumbling process and describes the cross-over between the two previous regimes. This knowledge, however, could allow to use DDM for accessing the average tumble rate, other than providing better estimates for the run properties, *e.g.* bacterial velocity fluctuations and distributions. Note, that for the sake of simplicity we neglect in this work the typical duration of a tumble event, that is, the tumbling process is assumed to be instantaneous. It has been shown that a finite tumble time leads to non-trivial corrections [5,6], and thus should be taken into account when aiming for a more quantitative description.

Mathematically, in the run-and-tumble model, the density distribution of the bacteria population obeys a kinetic equation in the form [4]

$$\partial_t f(\mathbf{r},\mathbf{v},t) = -v_0\,\hat{u}\cdot\partial_{\mathbf{r}}\, f(\mathbf{r},\mathbf{v},t) - \lambda\, f(\mathbf{r},\mathbf{v},t) + \frac{\lambda}{\Omega}\int \mathrm{d}\hat{u}'\, f(\mathbf{r},v_0\hat{u}',t), \quad (1)$$

[a] e-mail: lyderic.bocquet@univ-lyon1.fr

where $f(\mathbf{r}, \mathbf{v}, t)$ is the density distribution to get a bacteria with position $\mathbf{r}$ and velocity $\mathbf{v} = v_0\,\hat{u}$ at time t, v_0 is the self-propelling speed (here assumed to be a constant), $\hat{u}$ is the unit vector pointing to the direction of motion of the bacteria; Ω is the total solid angle, verifying $\Omega = \int \mathrm{d}\hat{u}'$. In the following, we introduce a projector operator $\mathbb{P}(\cdot) = \frac{1}{\Omega}\int \mathrm{d}\hat{u}'(\cdot)$. This equation is valid for any dimension of space. The ISF identifies with the Fourier transform of the projected distribution

$$F(k,t) = \int \mathrm{d}\mathbf{r}\ \mathbb{P}\cdot f(\mathbf{r}, v_0\,\hat{u}, t)\, e^{i\mathbf{k}\cdot\mathbf{r}}. \tag{2}$$

In this paper, we develop an exact expression for the density distribution and ISF. This is obtained by a formal analogy (in 3D) of the "run and tumble" model with the so-called Lorentz kinetic model, first introduced by Lorentz in 1905 to describe the motion of electrons in metals [13]. Accordingly the formal exact solution obtained by Hauge [14] for the Lorentz model provides an explicit formula for the density distribution of bacteria undergoing run and tumble dynamics. Results for the ISF for bacterial dynamics are discussed in this context. We then comment on the motion of bacteria close to boundaries on the basis of a formal analogy of the motion of electrons in a magnetic field.

2 Run-and-tumble and analogy with the Lorentz model

In the Lorentz model, one assumes that collisions between electrons can be neglected, while collisions with the atoms of the metal are described as collisions with hard spheres. Due to their large mass, the latter are assumed to act as immobile scatterers that are randomly distributed with a homogeneous density. The electrons thus perform ballistic motion separated by specular collisions occuring on randomly distributed atoms. This dynamics can be described in terms of a (linear) Boltzmann equation for the electron distribution, which writes in 3D

$$(\partial_t + \mathbf{v}\cdot\partial_{\mathbf{r}})f(\mathbf{r},\mathbf{v},t) = \pi\,\rho\,R^2|\mathbf{v}|(\mathbb{P}-1)f(\mathbf{r},\mathbf{v},t). \tag{3}$$

Here, ρ is the density of scattering atoms, R is the sum of the electron and atom radii; $\mathbb{P}$ is the projection operator defined above. One should note that the norm of the velocity $v_0 = |\mathbf{v}|$ is conserved by the dynamics, as collisions on the heavy atoms are specular. Therefore, eq. (3) is found to match exactly eq. (1) for the run-and-tumble dynamics. Physically, tumble events correspond in the Lorentz model to collisions of the electrons with the background atoms. Accordingly, the mean free time between collisions, $\epsilon = (\pi\,\rho\,R^2\,v_0)^{-1}$, corresponds to the inverse tumble rate: $\epsilon = \lambda^{-1}$.

Assuming the complete randomization of direction after a tumble the velocity correlation function at a time delay $t - t'$ will be simply given by v_0^2 times the probability of having no tumble events in a time interval $t - t'$:

$$\langle \mathbf{v}(t)\cdot\mathbf{v}(t')\rangle = v_0^2 e^{-\lambda\,|t-t'|}. \tag{4}$$

By double integration we can obtain an explicit expression for the mean square displacement

$$\langle|\mathbf{r}(t) - \mathbf{r}(0)|^2\rangle = \frac{2v_0^2}{\lambda^2}(\lambda t - 1 + e^{-\lambda\,t}), \tag{5}$$

which, as opposed to Brownian motion, has no dependence on the dimensionality of the space.

2.1 Exact solution to the run-and-tumble model

Following the derivation by Hauge for the Lorentz model in 3D [14] (here applied to any dimension for the run-and-tumble model), one introduces the Laplace-Fourier transform of the distribution $f(\mathbf{r}, \mathbf{v}, t)$:

$$\Phi(\mathbf{k},\mathbf{v},z) = \int_0^\infty \mathrm{d}t\ \exp(-zt)\int \mathrm{d}\mathbf{r}\exp(i\mathbf{k}\cdot\mathbf{r})\, f(\mathbf{r},\mathbf{v},t). \tag{6}$$

The Fourier transform of the initial distribution $f(\mathbf{r}, \mathbf{v}, t = 0)$ is denoted as $h(\mathbf{k}, \mathbf{v})$

$$h(\mathbf{k},\mathbf{v}) = \int \mathrm{d}\mathbf{r}\exp(i\mathbf{k}\cdot\mathbf{r})\, f(\mathbf{r},\mathbf{v},t=0). \tag{7}$$

As pointed out in ref. [14], the trick to obtain the exact solution for the above kinetic equation is that a closed equation on the projected distribution $\mathbb{P}\cdot f$ (Fourier-Laplace transformed) can be found and reinjected into the full equation.

Let us first introduce an orientationally averaged ballistic propagator, $P_0(\mathbf{k}, z)$, as

$$P_0(\mathbf{k},z) = \mathbb{P}\left(\frac{1}{z+\lambda - i\mathbf{k}\cdot\mathbf{v}}\right). \tag{8}$$

This corresponds to the ISF in the absence of tumbling events. It is straightforward to compute $P_0(k, t)$ for any dimension of the system:

$$\begin{aligned}
&\text{3D}: \ P_0(\mathbf{k},z) = \frac{1}{kv_0}\tan^{-1}\frac{kv_0}{z+\lambda}\,,\\
&\text{2D}: \ P_0(\mathbf{k},z) = [(z+\lambda)^2 + (kv_0)^2]^{-1/2},\\
&\text{1D}: \ P_0(\mathbf{k},z) = \frac{(z+\lambda)}{(z+\lambda)^2 + (kv_0)^2}\,,
\end{aligned} \tag{9}$$

The exact solution for an arbitrary initial condition is then obtained as

$$\begin{aligned}
\Phi(\mathbf{k},\mathbf{v},z) = {}& \frac{\lambda}{z+\lambda - i\mathbf{k}\cdot\mathbf{v}}\times\frac{1}{1-\lambda\,P_0(\mathbf{k},z)}\\
&\cdot\mathbb{P}\left(\frac{h}{z+\lambda-i\mathbf{k}\cdot\mathbf{v}}\right) + \frac{h}{z+\lambda-i\mathbf{k}\cdot\mathbf{v}}\,.
\end{aligned} \tag{10}$$

Now, we specialize to the case where the bacteria are initially located at a position $\mathbf{r} = 0$ with an arbitrary orientation $\hat{u}$, so that $f(\mathbf{r}, \mathbf{v}, t = 0) = \delta(\mathbf{r})$, and $h(\mathbf{k}, \mathbf{v}) = 1$. Then one obtains

$$\mathbb{P}\left(\frac{h}{z+\lambda-i\mathbf{k}\cdot\mathbf{v}}\right) = P_0(\mathbf{k},z), \tag{11}$$

so that the exact solution for the propagator $\Phi(\mathbf{k},\mathbf{v},z)$ takes the expression

$$\Phi(\mathbf{k},\mathbf{v},z) = \frac{1}{z+\lambda-i\mathbf{k}\cdot\mathbf{v}} \times \frac{1}{1-\lambda P_0(\mathbf{k},z)}\,. \qquad (12)$$

In order to obtain the ISF, one is interested in the probability $P(\mathbf{r},t)$ to find the particle at a position $\mathbf{r}$ at time t, which is obtained by averaging over the orientations of the velocity: $P(\mathbf{r},t) = \mathbb{P}\cdot f(\mathbf{r},\mathbf{v},t)$. One deduces the Laplace transform of the ISF

$$P(\mathbf{k},z) = \frac{P_0(\mathbf{k},z)}{1-\lambda\, P_0(\mathbf{k},z)}\,. \qquad (13)$$

Combining with the expressions for the ballistic operator in any dimension, eqs. (9), one obtains accordingly the analytical expression of the Laplace transform of the ISF in any dimension. It is interesting to remark that this result is identical to the one by Kolesnik for random motion [15], although the derivation based on the Lorentz analogy is more direct and straightforward.

One can get a physical picture of the dynamics by noting that this equation allows to rewrite the ISF as an infinite sum of collisions steps following ballistic propagation

$$P(\mathbf{k},z) = \sum_{n=0}^{\infty} \lambda^n\, P_0(k,z)^{n+1}. \qquad (14)$$

Alternatively, one may also interprete the above result in eq. (13) by writing the corresponding integral equation for the ISF in real time

$$P(\mathbf{k},t) = P_0(\mathbf{k},t) + \lambda \int_0^t \mathrm{d}s\, P_0(\mathbf{k},t-s)P(\mathbf{k},s). \qquad (15)$$

Formally, one can write a corresponding Dyson series, here associated with a collision expansion, and fully equivalent to eq. (14)

$$\begin{aligned} P(\mathbf{k},t) = P_0(\mathbf{k},t) &+ \lambda \int_0^t \mathrm{d}s\, P_0(\mathbf{k},t-s)P_0(\mathbf{k},s) \\ &+\lambda^2 \int_0^t \mathrm{d}s \int_0^s \mathrm{d}s'\, P_0(\mathbf{k},t-s)P_0(\mathbf{k},s-s')P_0(\mathbf{k},s') \\ &+ \dots\,. \end{aligned} \qquad (16)$$

This integral equation has a clear physical interpretation in terms of ballistic propagation, separated by collision steps leading to a gradual loss of memory.

2.2 Solution in various dimensions

2.2.1 Solution in 3D

Specializing to 3D, one gets explicitly

$$P(\mathbf{k},z) = \frac{\frac{1}{kv_0}\tan^{-1}\frac{kv_0}{z+\lambda}}{1-\frac{\lambda}{kv_0}\tan^{-1}\frac{kv_0}{z+\lambda}}\,. \qquad (17)$$

This result has interesting limiting behaviors. First for long time and small k, one can get the asymptotic expression, see *e.g.* [16]

$$P(\mathbf{k},z) \simeq \frac{1}{z+D_{\mathrm{eff}}k^2}\,, \qquad (18)$$

i.e. $P(\mathbf{k},t) \simeq \exp(-D_{\mathrm{eff}}k^2t)$, with the expression of the effective diffusion coefficient as $D_{\mathrm{eff}} = v_0^2/3\lambda$ in perfect agreement with the diffusive behavior at long time.

For short times ($z \to \infty$), an asymptotic expansion leads to the expression

$$P(\mathbf{k},t) \simeq \frac{\sin(kv_0t)}{kv_0\,t}\,. \qquad (19)$$

This is the Fourier transform of $P(\mathbf{r},t) = \frac{\delta(r-v_0t)}{4\pi r^2}$, *i.e.* a ballistic motion expanding spatially at constant velocity from the origin $r = 0$, as expected.

2.2.2 Analytical solutions in 2D

In two dimensions, the corresponding Laplace tansform of the ISF writes as

$$P(\mathbf{k},z) = \frac{[(z+\lambda)^2+(kv_0)^2]^{-1/2}}{1-\lambda[(z+\lambda)^2+(kv_0)^2]^{-1/2}}\,. \qquad (20)$$

In the hydrodynamic limit ($k \to 0, z \to 0$), one recovers $P(\mathbf{k},t) \simeq \exp(-D_{\mathrm{eff}}k^2t)$ with, for 2D, $D_{\mathrm{eff}} = v_0^2/2\lambda$, as expected.

Now, this 2D geometry allows to push analytical calculations further and obtain an analytical form for the ISF, as well as its counterpart in real space —the van Hove function. Indeed, for 2 dimensions, the inverse Laplace transform of $P_0(k,z)^{n+1}$ can be computed analytically as

$$\mathcal{L}^{-1}[P_0(k,z)^{n+1}] = \frac{\sqrt{\pi}}{2^{\frac{n}{2}}\,\Gamma(\frac{n+1}{2})} e^{-\lambda t}\left(\frac{t}{kv_0}\right)^{\frac{n}{2}} J_{\frac{n}{2}}(kv_0t), \quad (21)$$

with J_ν the Bessel function of the first kind and $\Gamma(x)$ the Euler gamma function. This allows to obtain an explicit expression for the ISF in terms of an infinite series

$$P(\mathbf{k},t) = e^{-\lambda\, t} \sum_{n=0}^{\infty} \frac{\sqrt{\pi}}{2^{\frac{n}{2}}\,\Gamma(\frac{n+1}{2})} \left(\frac{\lambda^2\, t}{k\, v_0}\right)^{\frac{n}{2}} J_{\frac{n}{2}}(k\, v_0\, t). \quad (22)$$

To obtain the van Hove function, one should compute the reverse Fourier transform of this sum

$$\begin{aligned} G_s(r,t) &= \int \frac{\mathrm{d}\mathbf{k}}{(2\pi)^2} e^{-i\mathbf{k}\cdot\mathbf{r}}\, P(\mathbf{k},t) \\ &= \frac{1}{2\pi}\int_0^\infty k\,\mathrm{d}k\, J_0(k\,r)P(k,t). \end{aligned} \qquad (23)$$

Using integral relationships on Bessel functions [17], one gets

$$\begin{aligned} G_s(r,t) = e^{-\lambda\, t}\Bigg[&\frac{\delta(r-v_0\,t)}{2\pi\, r} \\ &+ \sum_{n=1}^{\infty} \frac{\left(\frac{\lambda}{v_0}\right)^n \Delta(r,t)^{n-2}}{2^n\sqrt{\pi}\,\Gamma(\frac{n+1}{2})\,\Gamma(\frac{n}{2})}\Bigg] \end{aligned} \qquad (24)$$

for $r < v_0\,t$ and zero otherwise; $\Delta(r,t) = \sqrt{v_0^2 t^2 - r^2}$. The second term can be summed up exactly to give the final result

$$G_s(r,t) = e^{-\lambda\,t}\left[\frac{\delta(r - v_0\,t)}{2\pi r} + \frac{\lambda}{2\pi\,v_0\,\Delta(r,t)}\,e^{\frac{\lambda\,\Delta(r,t)}{v_0}}\right] \tag{25}$$

for $r < v_0\,t$ and 0 otherwise. It can be easily check that the above expression has the correct second moment (5). The solution matches the result obtained by Stadje [18] for two-dimensional random walks, and obtained by a very different method.

2.2.3 1D solutions

In 1D, the solution for the Laplace transform of the ISF is

$$P(\mathbf{k},z) = \frac{z+\lambda}{z\,(z+\lambda) + (k\,v_0)^2}\,. \tag{26}$$

One may check easily that the corresponding van Hove function in real space (inverse Laplace-Fourier transform of $P(\mathbf{k},z)$) obeys a telegrapher's equation in 1D

$$\frac{\partial^2}{\partial t^2}G(x,t) + \lambda\frac{\partial}{\partial t}G(x,t) = v_0^2\frac{\partial^2}{\partial x^2}G(x,t). \tag{27}$$

The solution of this equation is in full agreement with the result obtained in ref. [3] (with a factor of two in the definition of λ)

$$G(x,t) = \frac{e^{-\frac{\lambda\,t}{2}}}{2}\left(\delta(x - v_0 t) + \delta(x + v_0 t) + \frac{\lambda}{2v_0}\left[I_0\left(\frac{\lambda\Delta(x,t)}{2v_0}\right) + \frac{v_0\,t}{\Delta(x,t)}I_1\left(\frac{\lambda\Delta(x,t)}{2v_0}\right)\right]\right) \tag{28}$$

for $|x| < v_0\,t$ and 0 otherwise; $\Delta(x,t) = \sqrt{v_0^2 t^2 - x^2}$ as introduced above; I_0 and I_1 are modified Bessel functions.

3 Numerical results

In order to illustrate the use of the above results in typical experimental situations, we simulate the run-and-tumble dynamics of the self-propelled particles (see fig. 1) in a 2D infinite system. The equation of motion of a single particle is

$$\partial_t \mathbf{r}_n = v_0\hat{\mathbf{u}}_n, \tag{29}$$

with $\mathbf{r}_n$ the position of self-propelled particle n ($n \in [1,N]$), v_0 the constant speed, the same for all particles and $\hat{\mathbf{u}}_n$ the unit vector indicating the direction of motion of particle n. The direction is changed with rate λ.

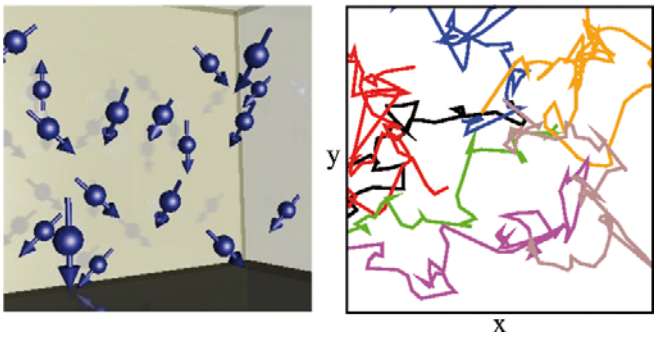

Fig. 1. Left: scheme of self-propelled particles in 3D. Left: typical 2D trajectories of self-propelled particles with run-and-tumble dynamics.

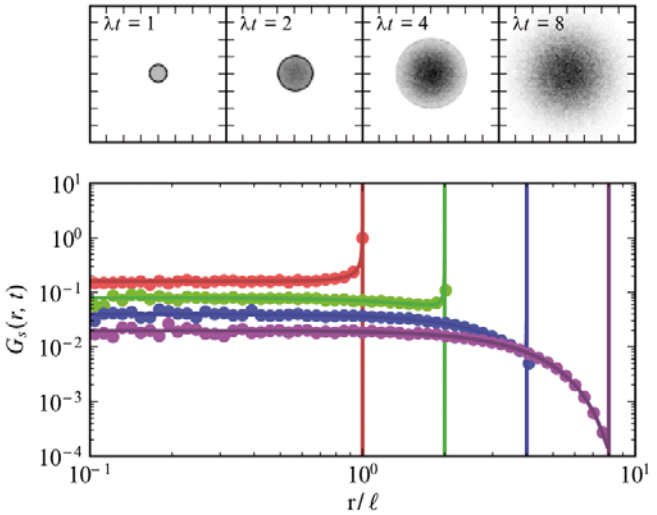

Fig. 2. Top: numerically evaluated particle distributions at four different times. At $\lambda t = 1$ a fraction $1/e$ of "ballistic" particles is still visible as a marked outer ring component. For the last plotted time $\lambda t = 8$ the ring is no longer visible and the distribution of particles tends to the limit Gaussian shape. Bottom: van Hove function $G_s(r,t)$ as a function of the rescaled distance r/ℓ at the four times reported on the top panel. Solid circles indicate numerically obtained values, compared to the analytical expression given in eq. (25) (solid lines).

The new direction is drawn from a uniform distribution. The average persistence length is thus given by $\ell = v_0/\lambda$. In non-dimensionless quantities we measure velocities in units of v_0 and times in units of $1/\lambda$.

We measure the density probability distribution, *i.e.* the van Hove function, in the simulations and compare to the analytical expression for the 2D van Hove function given in eq. (25). As shown in the bottom panel of fig. 2, the analytical prediction perfectly reproduces the numerically obtained curves. We note that a similar agreement is found in 1 and 3D as expected (not shown), although in the latter case only the Fourier-Laplace transform of the van Hove function is known and a numerical inversion of eq. (17) is performed.

4 Run and tumble near solid boundaries

An interesting extension of the previous analogy concerns the behavior of bacteria close to surfaces [19–22]. In this situation, bacteria follow circular trajectories at a given rotation velocity, say ω, and remain near the surface over long periods. This points to the important role of the motility of *E. coli* near surfaces on biolfilm formation and infections [20,23]. The origin of this circular motion is the hydrodynamic interaction between the bacteria and the surfaces, so that the sign of the rotation (clockwise *versus* anti-clockwise) depends on the nature of the hydrodynamic boundary condition at the surface [22]. Furthermore the amplitude of the rotation velocity is a complex function of the geometrical characteristics of the bacteria [20,22].

Now, one may consider how this circling motion affects the global dynamics of the bacteria, whenever tumbling motion is taken into account. We consider a bacteria undergoing a 2D motion in a plane close to a boundary, and characterized by a rotation velocity ω. Accordingly, one may generalize the run-and-tumble equation in order to account for the circular motion, as

$$\partial_t f(\mathbf{r},\mathbf{v},t) = -\partial_{\mathbf{r}}\left(v_0\,\hat{u} f(\mathbf{r},\mathbf{v},t)\right) - (\omega\times\mathbf{v})\cdot\partial_{\mathbf{v}} f(\mathbf{r},\mathbf{v},t) \\ -\lambda\, f(\mathbf{r},\mathbf{v},t) + \lambda\,\mathbb{P} f(\mathbf{r},\mathbf{v},t), \tag{30}$$

with $\mathbf{v} = v_0\hat{u}$, ω is the angular velocity along the direction perpendicular to the plane and $\mathbb{P}$ is the projection operator in the 2D plane defined above, $\mathbb{P}(.) = (2\pi)^{-1}\int \mathrm{d}\hat{u}\,(.)$.

Interestingly, this equation is the exact analog of the dynamics of an electron in a magnetic field (perpendicular to the plane), with ω the corresponding cyclotron frequency. In this case, an exact solution has been obtained (in 3D) by Cornu and Piasecki [24], see also ref. [16], and one may apply directly their method of derivation to the equation above (although here in 2D, the operator appearing in the equations in both problems are identical).

Following ref. [24], the Fourier-Laplace transform of the probability density $f_\omega(\mathbf{r},\mathbf{v},t)$ reads in this case

$$\Phi_\omega(\mathbf{k},\mathbf{v},z) = h_\omega(\mathbf{k},\mathbf{v},z) + \frac{\lambda\psi(\mathbf{k},\mathbf{v},z)}{1-\lambda\,\mathbb{P}\psi(\mathbf{k},\mathbf{v},z)}\times\mathbb{P}h_\omega(\mathbf{k},\mathbf{v},z), \tag{31}$$

with the effect of the initial state given by

$$h_\omega(\mathbf{k},\mathbf{v},z) = \int_0^\infty \mathrm{d}t\exp[-(z+\lambda)t \\ -i\mathbf{k}\cdot\mathbf{x}(\mathbf{v},t)]\hat{h}_\omega(\mathbf{k},\mathcal{R}_\omega(-\omega t)\cdot\mathbf{v}), \tag{32}$$

In this equation, $\hat{h}_\omega$ denotes the Fourier transform of the initial state $f_\omega(\mathbf{r},\mathbf{v},t=0)$ and $\mathcal{R}_\omega(\alpha)$ is the rotation of angle α around the axis in the direction of ω (perpendicular to the plane). The shorthand notation $\mathbf{x}(\mathbf{v},t) = \omega^{-1}[\mathcal{R}_\omega(\frac{\pi}{2}-\omega\,t)\cdot\mathbf{v} - \mathcal{R}_\omega(\frac{\pi}{2})\cdot\mathbf{v}]$ has been introduced and we have defined

$$\psi(\mathbf{k},\mathbf{v},z) = \int_0^\infty \mathrm{d}t\exp[-(z+\lambda)t - i\mathbf{k}\cdot\mathbf{x}(\mathbf{v},t)]. \tag{33}$$

Note that, in comparison to [24], only the 2D components in the plane (thus perpendicular to ω) are considered here. In order to compute the ISF, the initial condition $f_\omega(\mathbf{r},\mathbf{v},t=0) = \delta(\mathbf{r})$ is considered and $\hat{h}_\omega = 1$. The solution for the ISF is the projected function $P(\mathbf{k},z) = \mathbb{P}\cdot\Phi_\omega(\mathbf{k},\mathbf{v},z)$, and can be again written formally as

$$P(\mathbf{k},z) = \frac{P_0(\mathbf{k},z)}{1-\lambda\,P_0(\mathbf{k},z)}, \tag{34}$$

where P_0 defined here as $P_0 = \mathbb{P}\psi(\mathbf{k},\mathbf{v},z)$ is the orientationally averaged "ballistic" propagator, here associated with rotational motion. Using the previous definition in eq. (33), the angular integral involved in $\mathbb{P}\psi$ can be performed explicitly to give

$$P_0(\mathbf{k},z) = \int_0^\infty \mathrm{d}t\exp[-(z+\lambda)t]\,J_0\left(\frac{2kv}{\omega}\sin\frac{\omega\,t}{2}\right), \tag{35}$$

so that in real time, the projected propagator $P_0(\mathbf{k},t)$ takes the expression

$$P_0(\mathbf{k},t) = \exp[-\lambda t]\,J_0\left(\frac{2kv}{\omega}\sin\frac{\omega\,t}{2}\right). \tag{36}$$

As one expects, the latter result reduces to the previous expression for the propagator in the limit $\omega\to 0$, see eq. (21). While we could not push further the analytical calculations, the ISF can be formally calculated in terms of the collision expansion in eq. (16) with the "ballistic" operator now given in the equation above.

The long-time diffusive behavior can however be obtained from a low-k expansion of the ISF in eq. (34), in the form $P(\mathbf{k},z)\simeq(z+D_\omega k^2)^{-1}$. Formally this is obtained by computing the pole $z_{\mathrm{diff}}(k)$ in eq. (34), defined as $1/P_0(\mathbf{k},z_{\mathrm{diff}}(k)) = \lambda$. In the $k\to 0$ limit, one has $P_0(\mathbf{k},z) = \frac{1}{z+\lambda}\left(1-\frac{k^2\frac{v^2}{2}}{(z+\lambda)^2+\omega^2}\right)+\mathcal{O}(k^4)$, so that the asymptotic behavior of the pole in the limit $k\to 0$ takes the form

$$z_{\mathrm{diff}}(k)\simeq -D_\omega k^2 + \mathcal{O}(k^4), \tag{37}$$

where the expression for the diffusion coefficient now takes the expression

$$D_\omega = D_{\mathrm{eff}}\frac{1}{1+\omega^2\tau^2} \tag{38}$$

and $D_{\mathrm{eff}} = \frac{1}{2}v_0^2\tau$ is the bare 2D diffusion coefficient, and $\tau = \lambda^{-1}$.

We finally quote that the above result for the diffusion coefficient can be also obtained from a direct calculation of the velocity autocorrelation function in the presence of a rotational velocity. Following the same calculations as in ref. [24], one may indeed obtain

$$\langle v_\alpha(t)v_\alpha(0)\rangle = \frac{v_0^2}{2}\cos(\omega\,t)\,e^{-\lambda\,t}, \tag{39}$$

with $\alpha = \{x,y\}$ the coordinates in the plane. Note that this result is obtained by a straightforward generalization of the 3D calculation in ref. [24] to the present 2D planar situation. This expression could also be obtained directly

by noting that after a delay time t, the velocity correlation is given simply by $v_0 \times [v_0 \cos(\omega\, t)]$, times the probability of having no tumble event during this period, $e^{-\lambda\, t}$.

Then, the diffusion coefficients for bacteria in the plane can be deduced from the Green-Kubo relationship

$$D_\omega = \frac{1}{2} \sum_{\alpha=x,y} \int_0^\infty \mathrm{d}t\, \langle v_\alpha(t) v_\alpha(0) \rangle, \tag{40}$$

leading to $D_\omega = \frac{v^2 \tau}{2} \times (1 + \omega^2 \tau^2)^{-1}$, with $\tau = \lambda^{-1}$, in agreement with the previous hydrodynamic expansion.

Similarly the cross-correlation of the velocity can be also computed as $\langle v_x(t) v_y(0) \rangle = \frac{v_0^2}{2} \sin(\omega\, t)\, \exp[-\lambda\, t]$, so that an off-diagonal diffusion $D_{xy} = -D_{yx}$ is also predicted

$$D_{xy} = -D_{\mathrm{eff}} \frac{\omega \tau}{1 + \omega^2 \tau^2}\,. \tag{41}$$

Altogether the circular motion hinders the diffusion of the particles at surfaces, and thus favors possible adhesion to the surface to form a biofilm. It suggests to explore experimentally the connection between the apparent diffusion at surfaces and the observed rotational velocity.

5 Conclusion

To conclude, we have made use of an analogy between the run-and-tumble dynamics of bacterial motility with the Lorentz model of electron conduction in order to obtain analytical prediction for the intermediate scattering function. The model is then extended to account for the circular motion of bacteria close to boundaries. It shows that the effective diffusion of bacteria is reduced due to circling.

Beyond the present context, it is interesting to note that the problem shares an interesting analogy with the structure factor of polymers with persistence length [25], thereby allowing to provide some analytical predictions in this situation also.

LB thanks J. Piasecki for fruitful discussions about the Lorentz model and F. Detcheverry for pointing the references on the random motion. KM was supported by the Marie Curie FP7-PEOPLE-2009-IEF program. LA and RDL acknowledge support from MIUR-FIRB project RBFR08WDBE, Italian Institute of Technology under the Seed project BACT-MOBIL and CASPUR High Performance Computing initiatives.

References

1. H.C. Berg, *E. Coli In Motion* (Springer, New York, 2004).
2. H.C. Berg, D.A. Brown, Nature (London) **239**, 500 (1972).
3. H.G. Othmer, S.R. Dunbar, W. Alt, J. Math. Biol. **26**, 263 (1988).
4. M.J. Schnitzer, Phys. Rev. E **48**, 2553 (1993).
5. J. Tailleur, M.E. Cates, Phys. Rev. Lett. **100**, 218103 (2008).
6. J. Tailleur, M.E. Cates, EPL **86**, 60002 (2009).
7. R.W. Nash, R. Adhikari, J. Tailleur, M.E. Cates, Phys. Rev. Lett. **104**, 258101 (2010).
8. M.E. Cates, Rep. Prog. Phys. **75**, 042601 (2012).
9. J. Saragosti, V. Calvez, N. Bournaveas, B. Perthame, A. Buguina, P. Silberzan, Proc. Natl. Acad. Sci. U.S.A. **108**, 16235 (2011).
10. L. Angelani, A. Costanzo, R. Di Leonardo, EPL **96**, 68002 (2011).
11. L.G. Wilson, V.A. Martinez, J. Schwarz-Linek, J. Tailleur, G. Bryant, P.N. Pusey, W.C.K. Poon, Phys. Rev. Lett. **106**, 018101 (2011).
12. Vincent A. Martinez, Rut Besseling, Ottavio A. Croze, Julien Tailleur, Mathias Reufer, Jana Schwarz-Linek, Laurence G. Wilson, Martin A. Bees, Wilson C. K. Poon, `arXiv:1202.1702v1`.
13. H.A. Lorentz, Arch. Néerl. **10**, 336 (1905); see also H.A. Lorentz, Collected Papers, Vol. III (Martinus Nijhoff, The Hague, 1936).
14. E. Hauge, Phys. Fluids **13**, 1201 (1970).
15. A.D. Kolesnik, J. Stat. Phys. **131**, 1039 (2008).
16. Pavel L. Krapivsky, Sidney Redner, Eli Ben-Naim (Editors), *A Kinetic View of Statistical Physics* (Cambridge University Press, 2010).
17. We use relation 6.575, in I.S Gradshteyn, I.M. Ryzhik, *Table of integrals, series and products*, 6th ed. (Academic Press, San Diego, 2000). The term $n = 0$ needs a specific treatment, see 6.512 (8).
18. W. Stadje, J. Stat. Phys. **46**, 207 (1987).
19. Allison P. Berke, Linda Turner, Howard C. Berg, Eric Lauga, Phys. Rev. Lett. **106** 101, 038102 (2008).
20. E. Lauga, W.R. DiLuzio, G.M. Whitesides, H.A. Stone, Biophys. J. **90**, 400 (2006).
21. P.D. Frymier, R.M. Ford, H.C. Berg, P.T. Cummings, Proc. Natl. Acad. Sci. U.S.A. **92**, 6195 (1995).
22. R. Di Leonardo, D. Dell'Arciprete, L. Angelani, V. Iebba, Phys. Rev. Lett. **106**, 038101 (2011).
23. K.M. Ottemann, J.F. Miller, Mol. Microbiol. **24**, 1109 (1997).
24. F. Cornu, J. Piasecki, Physica A **370**, 591 (2006).
25. A.J. Spakowitz, Z.-G. Wang, Macromolecules **37**, 5814 (2004).